A Systematic Search for Structures, Stabilities, Electronic and Magnetic Properties of Silicon Doped Silver Clusters: Comparison with Pure Silver Clusters

Ya-Ru Zhao[a], Hai-Rong Zhang[b], Mei-Guang Zhang[a], Bao-Bing Zheng[a], and Xiao-Yu Kuang[c]

[a] Department of Physics and Information Technology, Baoji University of Arts and Sciences, Baoji 721016, China
[b] Department of Electrical and Electronic Engineering, Baoji University of Arts and Sciences, Baoji 721016, China
[c] Institute of Atomic and Molecular Physics, Sichuan University, Chengdu 610065, China

Reprint requests to Y.-R. Z.; E-mail: scu_zyr@163.com

Z. Naturforsch. **68a,** 327 – 336 (2013) / DOI: 10.5560/ZNA.2012-0117
Received September 10, 2012 / revised November 5, 2012 / published online January 23, 2013

The geometric structures, stabilities, electronic and magnetic properties of silicon doped silver clusters Ag_nSi ($n = 1-9$) have been systematically investigated by using meta-generalized gradient approximation (meta-GGA) exchange correlation Tao–Perdew–Staroverov–Scuseria (TPSS) functional. Due to the sp^3 hybridization, the lowest energy structures of doped clusters favour the three-dimensional structure. The silicon atom prefers to be located at the surface of the host silver clusters. The isomers that correspond to high coordination numbers of the Si–Ag bonds are found to be more stable. By analyzing the relative stabilities, the results show that the quadrangular bipyramid Ag_4Si structure is the most stable geometry for the Ag_nSi clusters. Meanwhile, the fragmentation energies, second-order difference of energies, difference of highest occupied and lowest unoccupied molecular orbital (HOMO–LUMO gaps), and total magnetic moments exhibit pronounced even–odd alternations. The largest hardness difference (2.24 eV) exists between the clusters Ag_4Si and Ag_5, which illustrates that the corresponding Ag_4Si cluster has dramatically enhanced chemical stability.

Key words: Ag–Si Cluster; Geometric Configuration; Density Functional Theory.

1. Introduction

Metallic clusters have been one of the most active areas of material science research because that gives us broadened views into the essence of atomic bonding in solids while greatly challenging our instinctive understanding [1, 2]. In particular, many chemists and physicsts have worked with growing interest on silver and doped silver clusters [3 – 7]. The major reason is due to the fact that they exhibit unique size and shape dependence and have promising applications in many areas such as chemical sensing [8], catalysis [9, 10], photochemical [11], absorbing organic materials, and heliotechnics [12, 13], as well as nanofabrication [14].

Experimentally, the silver dimer was examined by Beutel's group with two laser spectroscopic methods and they reported a bond length of 2.53 Å [15]. Scherer et al. observed the laser absorption spectra of the AgSi dimer by time-of-flight mass spectroscopy and studied the electronic states by theoretical calculation using the second-order multiconfigurational perturbation theory (CASPT2) [16]. Howard et al. [17] investigated the Ag_5 cluster and found that its single occupied molecular orbital (SOMO) includes $5s$, $4p$, and $4d$ atomic orbital contributions. Harb et al. [18] presented a joint experimental and theoretical investigation for the absorption spectra of silver clusters Ag_n ($4 \leq n \leq 22$). Besides, numerous theoretical studies were carried out on various aspects of geometric, electronic, and thermodynamic properties of pure and doped silver clusters. Many basic properties such as ionization potential, electron affinity, energy gap, and polarizability of silver clusters are determined by many groups [19 – 26]. Hou et al. [27] studied the geometric and electronic structure of neutral and anionic doped silver clusters, $Ag_5X^{0,-}$ with X = Sc, Ti, V, Cr, Mn, Fe, Co, and Ni. A density-functional theory (DFT) study of the structure and stability of coinage-metal aluminum com-

pounds $Ag_nAl^{(0,\pm1)}$ ($n = 1-7$) were performed by Liu and Jiang [28]. The results exhibit that the doping clusters are more stable than the corresponding pure silver clusters. In light of the previous work [29], the doped iron atom prefers to stay at the center of the Ag_nFe ($n \leq 15$) clusters. Moreover, numerous theoretical studies were carried out on various aspects of geometrical, electronic, and magnetic properties of doped silver clusters, such as Ag_nNi_m, Ag_nAu_m, Ag_nPd_m, and Ag_nY clusters [30–33].

However, to the best of our knowledge, no systematic studies on the structure and stability of Ag_nSi ($n = 1-9$) clusters have been carried out so far. An important question arises: how do the structures and properties of pure silver clusters differ from their equivalent doped silver clusters when a silicon atom is doped into the silver clusters? Therefore, in the present work, we set out to theoretically investigate a series of small size Ag_nSi clusters with $n = 1-9$ in order to probe systematically the behaviour and the evolution of their geometries, stability, electronic and magnetic properties.

2. Computational Details

The structure optimization, together with the frequency analyses of the Ag_nSi and Ag_{n+1} ($n = 1-9$) clusters, were performed by GAUSSIAN 03 program package [34]. In our calculations, the Tao–Perdew–Staroverov–Scuseria (TPSS) [35] meta-generalized gradient approximation (meta-GGA) functional was used instead of the traditional GGA functional. The effects of the basis set on the cluster have also been discussed by Maroulis and co-workers [36–38]. Taking time-consuming into account, the basis sets labeled GENECP are the combinations of LANL2TZ (f) [39] and 6−311+G (d) [40] basis sets, which are employed for the silver and silicon atoms, respectively. In order to check the validity of the computational method, we first carried out a comparison by employing different density functionals for small clusters AgSi, Ag_2, and Si_2. The results are listed in Table 1. One can see that the calculated results based on the TPSS functional are in good agreement with the experiment values [15, 16, 41, 42]. Specially, the theoretical values (1.94 eV, 1.74 eV, and 3.17 eV) of the dissociation energies are well closed to experimental results (1.88 eV, 1.66 eV, and 3.22 eV). The bond lengths by TPSS functional for the AgSi and Si_2 clusters are underestimated 0.4% and 3.6%, respectively. In searching for the lowest energy structures, lots of possible initial structures, which include one-, two-, and three-dimensional configurations, are considered, starting from the previous optimized Ag_n and Ag_nX geometries [5, 24–33], and all clusters are relaxed fully without any symmetry constraints. Towards nuclear displacement, all the structures have real vibrational frequencies and therefore correspond to the potential energy minima.

3. Results and Discussions

3.1. Bare Silver Clusters Ag_n ($n = 2-10$)

To investigate the effects of the silicon atom on silver clusters, we first perform some optimizations and discussions on pure silver clusters Ag_n ($n = 2-10$) by using the TPSS method and LANL2TZ (f) basis set. In light of the previous works [5, 20, 21], one can find that the ground state structures (shown in Figure 1) for Ag_n ($n = 2-10$) clusters are in good agreement with the previous results except for Ag_9. For Ag_9 clusters, a more recent theoretical work [20] has shown that a tri-capped rectangular bipyramid structure is the

Table 1. Calculated and experimental bond lengths r, dissociation energies D_e, and frequencies ω_e for the AgSi, Ag_2, and Si_2 clusters.

Methods	AgSi			Ag_2			Si_2		
	r [Å]	D_e [eV]	ω_e [cm^{-1}]	r [Å]	D_e [eV]	ω_e [cm^{-1}]	r [Å]	D_e [eV]	ω_e [cm^{-1}]
B3LYP	2.42	1.72	276.0	2.74	1.54	176.0	2.28	3.06	485.5
B3PW91	2.41	1.71	284.4	2.59	1.48	182.9	2.27	3.13	497.1
PW91PW91	2.38	2.06	293.1	2.58	1.78	185.7	3.22	3.38	468.8
PBEPBE	2.39	2.04	292.5	2.58	1.77	183.2	2.30	3.37	468.8
BP86	2.38	2.05	292.4	2.58	1.74	186.2	2.30	3.37	465.6
TPSSTPSS	2.39	1.94	290.8	2.57	1.74	189.5	2.17	3.17	539.3
Experiment	2.40[a]	1.88[a]	297.0[a]	2.53[b]	1.66[b]	192.0[c]	2.25[d]	3.22[d]	511.0[d]

[a] [16], [b] [15], [c] [41], [d] [42].

most stable structure. However, Zhao et al. [43] and Bonačić-Koutecký et al. [19] obtained a bi-capped pentagonal bipyramid structure as their ground state. In our calculations, the tri-capped bipyramid structure is 0.07 eV higher in total energy than the bi-capped pentagonal bipyramid structure. Moreover, the value (5.31 eV) of vertical ionization potential for the latter is much more close to experimental data (5.15 eV) comparison with that (5.86 eV) for the former.

3.2. Silicon–Silver Clusters Ag_nSi ($n = 1-9$)

In Figure 1, we show the lowest energy isomers and few low-lying structures of the Ag_nSi ($n = 1-9$) clusters for each size. Meanwhile, the symmetries, electronic states, and energy gaps for all isomers are listed in Table 2. The triangular structure (2a) with C_{2v} symmetry is the ground state isomer, which has a 76.1° angle, and two 2.40 Å of Ag–Si bonds. For Ag_3Si clusters, a dibridged structure (3a) with C_s symmetry is found to be the most stable structure. When the silver atom is bi-capped to the 2a isomer, a stable isomer (3c) is obtained. Although 3c has the highest gap of 0.91 eV, its total energy is higher than that of 3a by 1.011 eV. Our calculations reveal that the quadrangular structure (4a), with $^1A_1$ electronic state and identical 2.51 Å bonds of Ag–Si, is the lowest energy isomer of the Ag_4Si clusters. After the silver atoms are capped on the 3b isomer, two derived isomers (4b and 4c) are generated. It is interesting that the Ag–Si bond length elongates to 2.45 Å in the 4b isomer, whereas it shortens to 2.38 Å in 4c. The reason may be that the capped silver atom in 4b pushes surrounding silver atoms but it attracts them in the 4c isomer. As calculated previously by Kiran et al. [44] and Cao et al. [45], the tetrahedral isomer with T_d symmetry is the ground state structure for neutral Au_4Si clusters. However, this structure (4c) for Ag_4Si clusters is less stable than the quadrangular pyramidal structure (4a). With regard to the Ag_4Si clusters, three derived isomers (5a, 5c, and 5e) are obtained after one silver capping on different sites of the quadrangular pyramid structure (4a). In them, we find that the quadrangular bipyramid structure 5a is more stable than 5c and 5e because 5a is 0.130 eV and 0.316 eV in total energy lower than 5c and 5e, respectively. Amazedly, the same fact appeared for the 4b and 4c isomers occurs with the 5a and 5e structures. The bond length of Ag–Si elongates to 2.56 Å from 2.51 Å in the 5a isomer but shortens to 2.50 Å in 5e. As for Ag_6Si clusters, the most stable structure 6a can be yielded by tri-capping the silver atom on the 5c isomer. Among four derived structures of the 5a isomer, 6b is generated when the sixth silver atom is bi-capped on the side of the 5a isomer, and the 6c isomer is formed

Table 2. Relative energies ΔE, symmetries, electronic states, and HOMO–LUMO gaps E_g of the lowest energy and few low-lying Ag_nSi ($n = 1-9$) clusters.

Isomers	ΔE	symmetry	state	E_g
1a	0	$D_{\infty h}$	—	0.78
2a	0	C_{2v}	$^1A_1$	0.90
2b	2.311	$D_{\infty h}$	$^5\Sigma_u$	1.18
2c	2.394	$C_{\infty v}$	$^5\Sigma$	1.51
3a	0	C_s	$^2A'$	0.83
3b	0.447	C_{3v}	$^2A_1$	0.19
3c	1.011	C_s	$^2A_1$	0.91
4a	0	C_{4v}	$^1A_1$	2.54
4b	0.232	C_{3v}	$^1A_1$	2.31
4c	0.980	C_{3v}	$^1A_1$	1.83
4d	1.431	C_1	^3A	0.66
4e	1.625	C_{2v}	$^3B_2$	1.24
5a	0	C_{4v}	$^2A_1$	0.65
5b	0.087	C_s	$^2A'$	0.42
5c	0.130	C_s	$^2A'$	0.49
5d	0.278	C_s	^2A	0.47
5e	0.316	C_{4v}	$^2A_1$	0.37
5f	1.442	C_s	$^2A'$	0.44
6a	0	C_s	$^1A'$	1.75
6b	0.139	C_s	$^1A'$	1.12
6c	0.168	C_s	$^1A'$	0.87
6d	0.259	C_{4v}	$^1A_1$	1.51
6e	0.295	C_s	^1A	1.53
6f	0.299	C_{4v}	$^1A_1$	1.51
6g	0.496	C_{2v}	$^1A_1$	0.54
7a	0	C_s	$^2A'$	0.43
7b	0.003	C_1	^2A	0.42
7c	0.003	C_1	^2A	0.42
7d	0.047	C_{2v}	$^2B_2$	0.42
7e	0.100	C_s	$^2A''$	0.40
7f	0.198	C_s	$^2A'$	0.41
7g	0.256	C_1	^2A	0.35
8a	0	C_s	$^1A'$	1.02
8b	0.076	C_s	$^1A'$	1.07
8c	0.147	C_s	$^1A'$	0.94
8d	0.153	C_s	$^1A'$	0.87
8e	0.180	C_s	$^1A'$	1.00
8f	0.210	C_1	^1A	0.83
8g	0.228	C_{2v}	$^1A_1$	0.48
8h	0.401	C_s	$^1A'$	1.00
9a	0	C_s	$^2A''$	0.37
9b	0.054	C_s	$^2A'$	0.30
9c	0.162	C_1	^2A	0.31
9d	0.247	C_{2v}	$^2B_1$	0.36
9e	0.289	C_s	$^2A'$	0.31
9f	0.376	C_s	$^2A'$	0.35
9g	0.582	C_{2v}	$^2A_1$	0.37
9h	0.604	C_s	$^2A'$	0.42

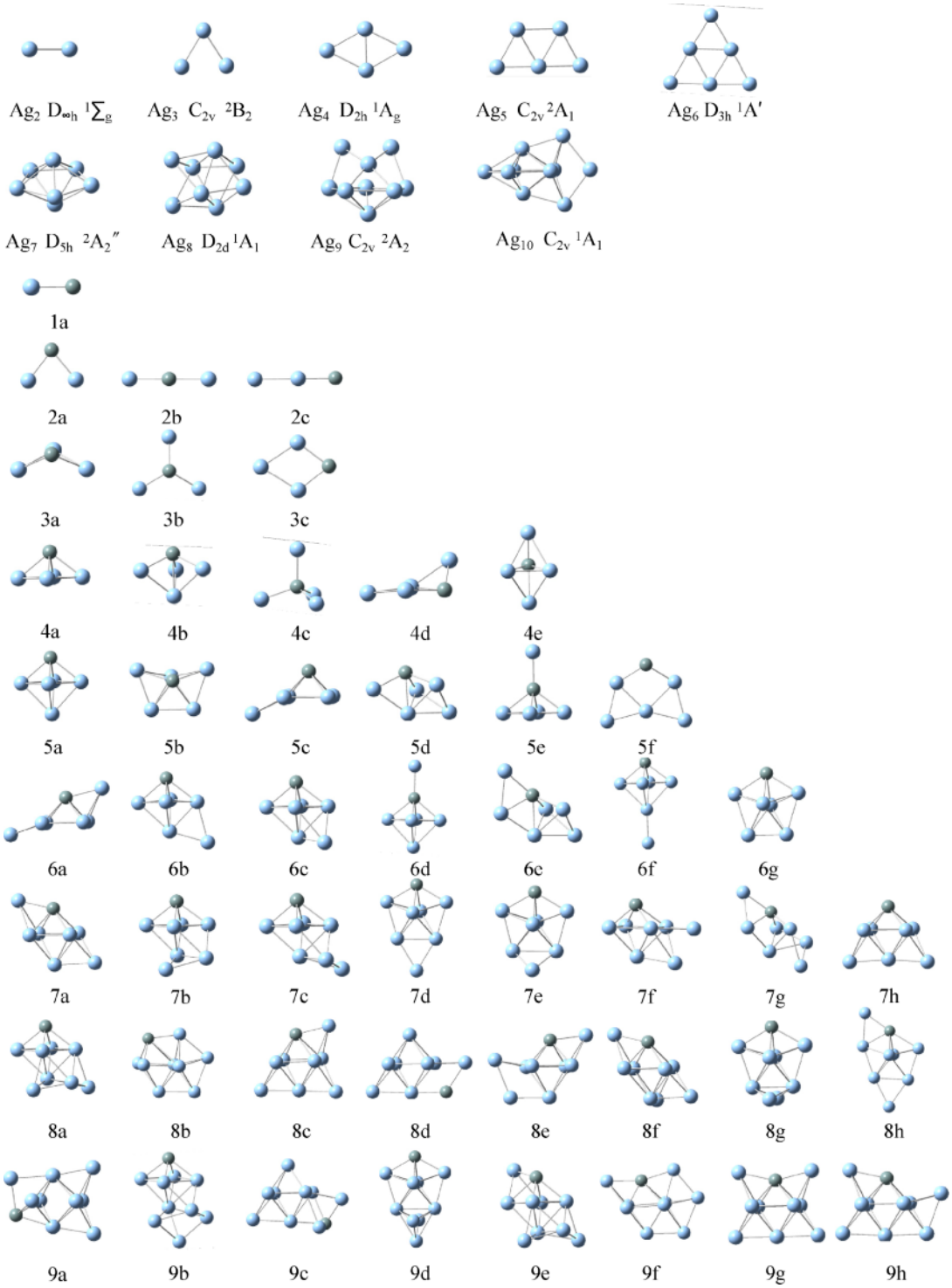

Fig. 1 (colour online). Lowest energy structures of pure silver clusters for each size; the lowest energy and few low-lying structures of Ag_nSi ($n = 1-9$) clusters. The argent and grey balls represent silver and silicon atoms, respectively.

after it is edge-capped on 5a; high symmetry isomers 6d and 6f are yielded when the silver atoms are top-capped and bottom-capped on the 5a structure, respectively. When the silver atoms are capped on the 6c isomer, the most stable structure 7a and three low-lying isomers 7b, 7c, and 7f evolve. From Table 2, one can see that 7a is a little more stable than the 7b and 7c isomers; the energy differences are 0.003 eV. Taking the energy gaps into account, 7a can be viewed as the most stable structure of Ag_7Si clusters. In the case of ground states, isomer 8a can be described as one silver atom being right-capped on the 7b structure and also viewed as one silver atom being left-capped on the 7c cluster. In optimized structures, isomers 8b and 8c can be viewed as two substituted structures of the most stable Ag_9 clusters reported by Fournier [22] and Huda and Ray [20]. On the basis of the 8a clusters, two isomers (9b and 9e) can be optimized. Furthermore, we have obtained the substituted structure (9d) of ground state Ag_{10} clusters. However, the total energies reveal that all of them are less stable than the new structure (9a), and the relative energies for them compared with 9a are 0.054 eV, 0.289 eV, and 0.247 eV, respectively.

It is concluded that the lowest energy structures of Ag_nSi clusters for $n > 2$ favour the three-dimensional structure due to the sp^3 hybridization of the silicon atom. From $n > 2$, the lowest energy structures of Ag_nSi clusters are not similar structures to those of the pure silver clusters. It indicates that the doped silicon atom dramatically affects the geometries of the ground state of Ag_n clusters. The isomers that correspond to high coordination numbers of Si–Ag bonds are found to be more stable. The doped silicon atom prefers to occupy the surface site of the Ag_nSi clusters, which is different from the fact of iron doped silver clusters [29].

3.3. Relative Stabilities

To predict the stability and size-dependent physical properties of clusters, the averaged atomic binding energies $E_b(n)$, fragmentation energies $\Delta E(n)$, and the second-order difference of energies $\Delta_2 E(n)$ are calculated. For the Ag_nSi clusters, $E_b(n)$, $\Delta E(n)$, and $\Delta_2 E(n)$ are defined as

$$E_b(n) = [nE(Ag) + E(Si) - E(Ag_nSi)]/(n+1), \quad (1)$$

$$\Delta E(n) = E(Ag_{n-1}Si) + E(Ag) - E(Ag_nSi), \quad (2)$$

$$\Delta_2 E(n) = E(Ag_{n-1}Si) + E(Ag_{n+1}Si) - 2E(Ag_nSi), \quad (3)$$

where $E(Ag_{n-1}Si)$, $E(Ag)$, $E(Si)$, $E(Ag_nSi)$, and $E(Ag_{n+1}Si)$ denote the total energy of the $Ag_{n-1}Si$, Ag, Si, Ag_nSi, and $Ag_{n+1}Si$ clusters, respectively.

For Ag_n clusters, $E_b(n)$, $\Delta E(n)$, and $\Delta_2 E(n)$ are defined by the following formula:

$$E_b(n) = [nE(Ag) - E(Ag_n)]/n, \quad (4)$$

$$\Delta E(n) = E(Ag_{n-1}) + E(Ag) - E(Ag_n), \quad (5)$$

$$\Delta_2 E(n) = E(Ag_{n-1}) + E(Ag_{n+1}) - 2E(Ag_n), \quad (6)$$

where $E(Ag_{n-1})$, $E(Ag)$, $E(Ag_n)$, and $E(Ag_{n+1})$ denote the total energy of the Ag_{n-1}, Ag, Ag_n, and Ag_{n+1} clusters, respectively.

To confirm the stability of the doped clusters, we also calculated the energy differences $E_{dis}(n)$ of Si, Ag_n, and Ag_nSi, clusters, defined as

$$E_{dis}(n) = E(Si) + E(Ag_n) - E(Ag_nSi). \quad (7)$$

With the use of above formulas, the calculated $E_b(n)$, $\Delta E(n)$, $\Delta_2 E(n)$, and $E_{dis}(n)$ values of the lowest energy Ag_nSi and Ag_{n+1} ($n = 1-9$) clusters are plotted in Figures 2a, b, c, and d. Firstly, the averaged atomic binding energies of the Ag_nSi clusters rises distinctly at $n = 1-4$, and show slight odd–even oscillations with increasing cluster size from $n > 4$. One visible peak occurs at $n = 4$, indicating that the Ag_4Si isomer is relatively more stable. Secondly, Figure 2a illustrates that the $E_b(n)$ values of Ag_nSi clusters are higher than those of Ag_{n+1} clusters, which hints that the impurity silicon atoms can enhance the stability of the pure silver clusters. Thirdly, the fragmentation energies and the second-order difference of energies of Ag_nSi clusters exhibit obvious odd–even alternations, which means that Ag_nSi clusters containing even-number silver atoms have higher relative stability than their neighbours. Furthermore, the calculated fragmentation energies and second-order difference energies for pure and doped clusters show an opposite trend. The reason may be that Ag_nSi clusters containing even-number silver atoms have paired *s* valence electrons while corresponding Ag_{n+1} clusters have unpaired ones. Lastly, it is found in Figures 2b and c that the Ag_4Si isomer corresponds to the local maxima of $\Delta E(n)$ and $\Delta_2 E(n)$ for doped silver clusters, which are 2.69 eV and 1.40 eV, respectively. It reveals that the Ag_4Si isomer possesses more stability. Furthermore, from Figure 2d, one can find a pyramid-like tendency in the region of $n = 1-8$ for Ag_nSi clus-

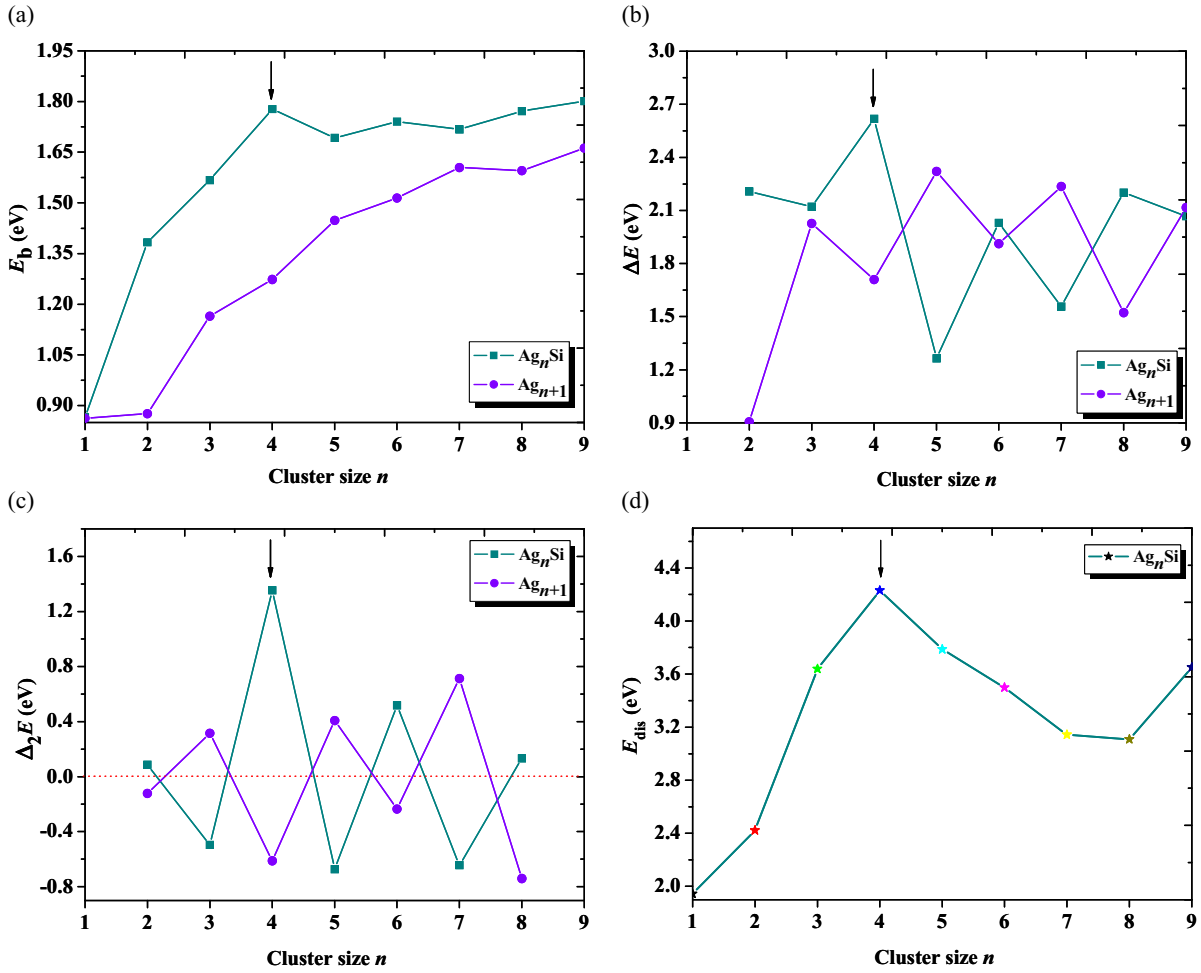

Fig. 2 (colour online). Size dependence of (a) the atomic average binding energies, (b) the fragmentation energies, (c) the second-order difference of energies for the lowest energy structures of Ag_nSi and Ag_{n+1} ($n = 1-9$) clusters, and (d) the energy differences of the lowest energy structures of Ag_nSi clusters.

ters, meanwhile, the conspicuous maximum appears at $n = 4$.

3.4. HOMO–LUMO Gaps and Charge Transfer

The highest occupied – lowest unoccupied molecular orbital (HOMO–LUMO) energy gap can provide an important criterion to reflect the chemical stability of clusters. For the lowest energy of the Ag_nSi ($n = 1-9$) clusters, the HOMO–LUMO gaps for the most stable Ag_nSi and Ag_{n+1} clusters against the cluster size are plotted in Figure 3. The trend of the Ag_nSi and Ag_{n+1} clusters show a contrary odd–even oscillation similar to $\Delta E(n)$ and $\Delta_2 E(n)$, which implies that $Ag_{2,4,6,8}Si$ and $Ag_{3,5,7,9}$ clusters have an enhanced stability compared with their neighbour clusters. Interestingly, the significant peak is also localized at $n = 4$ and the Ag_4Si isomer has the largest HOMO–LUMO gap of 2.54 eV. That means that the Ag_4Si cluster possesses a dramatically enhanced chemical stability. The reason may be that eight valence electrons of the Ag_4Si isomer form four identical Ag–Si covalent bonds. In addition, the HOMO and LUMO molecular orbitals of the Ag_4Si isomer include a sp^3 hybridization between the silver and silicon atoms. The natural population analysis (NPA) on the Ag_nSi ($n = 1-9$) clusters can provide re-

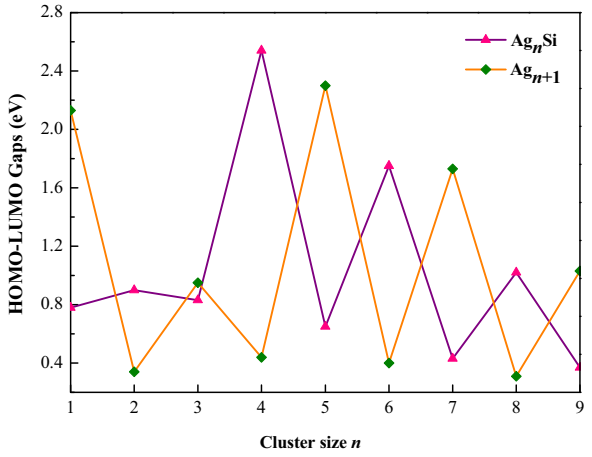

Fig. 3 (colour online). Size dependence of the HOMO–LUMO gaps for the lowest energy structure of Ag_nSi and Ag_{n+1} ($n = 1-9$) clusters.

liable charge-transfer (CT) information. Therefore, the results are summarized in Table 3. The silicon atoms possess negative charges from -0.128 to -0.817 e for $n = 2-9$, suggesting that the charges in the corresponding clusters transfer from the Ag_n frames to the silicon atom owing to a larger electron-negativity of the silicon than silver atom. However, the charges of the silicon atoms for AgSi isomers have 0.003 electrons, which means that the silicon atoms act as electron donor in the AgSi dimer. In addition, aiming at probing into the internal charge transfer in details, the natural electron configurations of impurity atoms and Ag_n frames are taken into account and these are tabulated in Table 4. For silicon atoms, it is shown that the $3s$ states lose $0.36-0.06$ electrons, while the $3p$ states get $0.05-1.11$ electrons. The contribution of $4p$ and $5p$ states is nearly zero. For silver atoms, the $5s$ orbitals lose $1.50-0.92$ electrons, while the $5p$ states get $0.04-0.88$ e charges. The values of $9.88-9.94$ electrons occupying the $4d$ subshell of the atoms reveal that the d obitals are dominant core obitals of silver atoms in Ag_nSi clusters.

3.5. Vertical Ionization Potential, Vertical Electron Affinity, and Chemical Hardness

The electronic properties of clusters can be reflected by the vertical ionization potential (VIP), the vertical electron affinity (VEA), and the chemical hardness. All of them are the most important characteristics, reflecting the size-dependent relationships of the electronic structure in cluster physics. Among them, VIP and VEA can be defined as

Table 3. Natural charges populations of the silicon and silver atoms for the lowest energy Ag_nSi ($n = 1-9$) clusters.

Clusters	Si	Ag(1)	Ag(2)	Ag(3)	Ag(4)	Ag(5)	Ag(6)	Ag(7)	Ag(8)	Ag(9)
AgSi	0.0026	−0.0026								
Ag_2Si	−0.1276	0.0638	0.0638							
Ag_3Si	−0.5494	0.2372	0.2372	0.0749						
Ag_4Si	−0.7431	0.1858	0.1858	0.1858	0.1858					
Ag_5Si	−0.5726	0.1501	0.1506	0.1506	0.1501	−0.0287				
Ag_6Si	−0.8173	0.0727	0.1975	0.2503	0.1975	0.0727	0.0265			
Ag_7Si	−0.6484	0.0978	0.1067	0.0478	0.0478	0.1067	−0.0432	0.2849		
Ag_8Si	−0.5366	0.1920	0.2817	−0.0394	0.1920	0.2817	0.0216	−0.3535	0.2849	
Ag_9Si	−0.4683	0.2405	−0.1826	−0.3178	−0.1826	0.3029	−0.1810	0.2405	−0.3535	0.2504

Table 4. Natural electron configurations (NEC) of silicon and silver atoms for the lowest energy Ag_nSi ($n = 1-9$) clusters.

Clusters	NEC (Si)	NEC (Ag)
AgSi	[core]$3s^{1.94}3p^{2.05}3d^{0.01}$	[core]$5s^{1.08}4d^{9.88}5p^{0.04}$
Ag_2Si	[core]$3s^{1.87}3p^{2.24}3d^{0.01}$	[core]$5s^{0.96}4d^{9.89}5p^{0.08}$
Ag_3Si	[core]$3s^{1.80}3p^{2.73}3d^{0.01}4p^{0.01}$	[core]$5s^{0.76-0.82}4d^{9.91}5p^{0.09-0.20}$
Ag_4Si	[core]$3s^{1.75}3p^{2.96}3d^{0.01}5s^{0.01}5p^{0.01}$	[core]$5s^{0.73}4d^{9.92}5p^{0.16}$
Ag_5Si	[core]$3s^{1.71}3p^{2.83}4s^{0.01}3d^{0.01}4p^{0.01}$	[core]$5s^{0.67-0.93}4d^{9.92-9.94}5p^{0.17-0.27}$
Ag_6Si	[core]$3s^{1.67}3p^{3.11}3d^{0.01}4p^{0.01}5s^{0.01}5p^{0.01}$	[core]$5s^{0.65-1.02}4d^{9.91-9.94}5p^{0.02-0.37}$
Ag_7Si	[core]$3s^{1.64}3p^{2.98}4s^{0.01}3d^{0.01}4p^{0.01}$	[core]$5s^{0.50-0.91}4d^{9.90-9.93}5p^{0.07-0.45}6p^{0-0.01}$
Ag_8Si	[core]$3s^{1.67}3p^{2.85}3d^{0.01}5p^{0.01}$	[core]$5s^{0.56-0.83}4d^{9.90-9.93}5p^{0.04-0.88}6p^{0-0.01}$
Ag_9Si	[core]$3s^{1.66}3p^{2.78}3d^{0.01}4p^{0.01}$	[core]$5s^{0.58-0.76}4d^{9.89-9.94}5p^{0.07-0.74}6p^{0-0.01}$

$$\mathrm{VIP} = E_{\text{cation at optimized neutral geometry}} - E_{\text{optimized neutral}}\,, \tag{8}$$

$$\mathrm{VEA} = E_{\text{optimized neutral}} - E_{\text{anion at optimized neutral geometry}}\,. \tag{9}$$

In Table 5, we have calculated VIP and VEA of the Ag_nSi and Ag_{n+1} clusters. From the table, one can see that the values of VIP and VEA for Ag_{n+1} clusters show an obvious contrary oscillating behaviour. It is noted that our calculated values of VIP agree well with experimental date as expected [46, 47]. When silicon atoms are doped into silver clusters, the strict odd–even oscillation behaviour of VIP for doped clusters is not found. In other words, primary electronic properties of silver clusters are destroyed duo to the effect of dopants. Especially, the Ag_4Si isomer shows the largest VIP of 7.30 eV.

In density functional theory, the chemical hardness η is expressed as

$$\eta = \mathrm{VIP} - \mathrm{VEA}\,. \tag{10}$$

Here, the hardness for Ag_nSi and Ag_{n+1} ($n = 1-9$) clusters have also been listed in Table 5, and the relationships of η vs. n are plotted in Figure 4. From $n = 3$, one can find that the hardness for Ag_{n+1} clusters still show odd–even oscillations. However, similar oscillatory tendency in the variation is not found for doped clusters. For the doped isomers, the values of η for Ag_4Si, Ag_6Si, and Ag_8Si clusters are higher than those of Ag_5, Ag_7, and Ag_9 clusters. The results indicate that the silicon atoms can enhance the chemical stability of the corresponding silver clusters. In particular, the largest hardness difference (2.24 eV) exists between the clusters Ag_4Si and Ag_5, which illustrates that the corresponding Ag_4Si cluster has dramatically enhanced chemical stability.

Table 5. Vertical ionization potential, vertical electron affinity, and chemical hardness of the lowest energy Ag_nSi and Ag_{n+1} ($n = 1-9$) clusters.

Cluster	Ag_nSi			Ag_{n+1}			
size	η	VEA	VIP	η	VEA	VIP	VIP [46,47]
$n = 1$	6.66	0.62	7.28	6.92	0.81	7.73	7.60
$n = 2$	5.48	1.62	7.20	5.59	0.17	5.76	5.66
$n = 3$	5.10	1.54	6.64	5.00	1.43	6.43	6.65
$n = 4$	6.49	0.81	7.30	4.25	1.84	6.09	6.35
$n = 5$	5.58	1.07	6.65	6.08	1.16	7.24	7.15
$n = 6$	5.23	1.08	6.31	4.13	1.73	5.86	5.69
$n = 7$	3.85	1.54	5.49	5.33	1.30	6.63	7.10
$n = 8$	4.52	1.64	6.16	3.67	1.64	5.31	5.15
$n = 9$	3.78	1.88	5.66	4.39	1.40	5.79	6.25

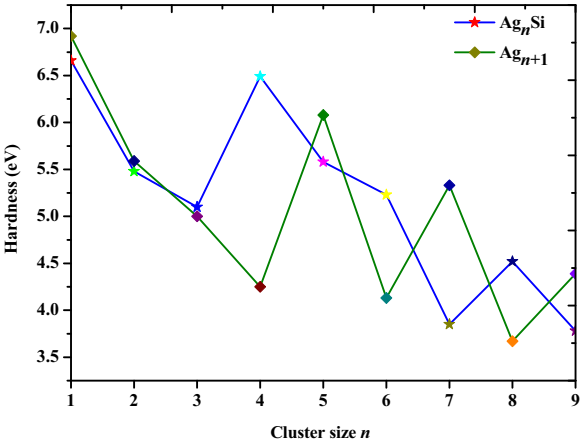

Fig. 4 (colour online). Size dependence of the chemical hardness for the lowest energy structures Ag_nSi and Ag_{n+1} ($n = 1-9$) clusters calculated.

3.6. Magnetic Moments

Based on the lowest energy structure, we further study the size evolution of the magnetic moment of

Table 6. Local magnetic moment of 3s, 3p, and 4s spin states of the silicon atom, 5s, 4d, and 5p spin states of the silver atoms in the lowest energy Ag_nSi ($n = 1-9$) clusters, and the total magnetic moment of the lowest energy Ag_nSi ($n = 1-9$) clusters.

Isomers		AgSi	Ag_2Si	Ag_3Si	Ag_4Si	Ag_5Si	Ag_6Si	Ag_7Si	Ag_8Si	Ag_9Si
Si	3s	0.01	0	0.02	0	0.01	0	0.03	0	0
	3p	0.99	0	0.75	0	0.44	0	0.24	0	0.34
	4s	0	0	0	0	0	0	0	0	0
	Sum	1.00	0.00	0.77	0.00	0.45	0.00	0.27	0.00	0.34
Ag_n	5s	−0.04	0	0.12	0	0.40	0	0.47	0	0.36
	4d	0.02	0	0.04	0	0.04	0	0.06	0	0.03
	5p	0.02	0	0.04	0	0.09	0	0.24	0	0.23
	Sum	0.00	0.00	0.20	0.00	0.53	0.00	0.77	0.00	0.72
Ag_nSi		1.00	0.00	0.97	0.00	0.98	0.00	1.04	0.00	1.06

the Ag_nSi clusters. The total magnetic moments as well as the local magnetic moments from the silicon atom and the Ag_n frames in Ag_nSi clusters are listed in Table 6. From the table, the primary features are concluded. Firstly, for the total magnetic moments of the Ag_nSi ($n = 1-9$) clusters exist distinctly odd–even alternation behaviours. For $Ag_{1,3,5,7,9}Si$ clusters, the total magnetic moment is close to $1\mu_B$ whereas for $Ag_{2,4,6,8}Si$ clusters, the values are zero. Secondly, the local magnetic moments from the silicon atoms and the Ag_n frames in corresponding Ag_nSi clusters shown the same odd–even behaviour. In $Ag_{2,4,6,8}Si$ clusters, for the contribution of the local magnetic moments from the silicon atoms exists a decreasing tendency, contrarily, that from Ag_n frames increases. Thirdly, the local magnetic moment comes mainly from the contribution of the $3p$ state for the silicon atoms and $5s$ and $5p$ states for silver atoms.

4. Conclusions

The results are summarized as follows:

(i) Due to the sp^3 hybridization of silicon atoms, the lowest energy structures of doped clusters favour the three-dimensional structure. The optimized geometries sh ow that the silicon atom prefers to occupy the surface site of the Ag_nSi clusters.

(ii) By analyzing the relative stabilities of the Ag_nSi ($n = 1-9$) clusters, we found that the Ag_4Si isomer shows the strongest stability due to its local peak in all the curves of $E_b(n)$, $\Delta E(n)$, $\Delta_2 E(n)$, $E_{dis}(n)$, and HOMO–LUMO gaps. The HOMO–LUMO gaps show a contrary odd–even oscillation, which implies that $Ag_{2,4,6,8}Si$ and $Ag_{3,5,7,9}$ clusters have enhanced stability compared with their neighbours.

(iii) The charges in Ag_nSi ($n = 1-9$) clusters transfer from the Ag_n frames to the silicon atom. For each silicon atom, the internal charges transfer from the $3s$ orbital to the $3p$ state. The contribution of the $4p$ and $5p$ states is nearly zero. Moreover, the results of VIP and hardness reveal that the Ag_4Si isomer has a dramatically enhanced chemical stability.

(iv) Pronounced odd–even oscillations are found for the total magnetic moment of Ag_nSi ($n = 1-9$) clusters. The local magnetic moment mainly arises from the contribution of the $3p$ state for silicon atoms and the $5s$ and $5p$ states for silver atoms.

Acknowledgements

This work was supported by the Natural Science Foundation of China (No. 11204007), the Natural Science Basic Research Plan in Shaanxi Province of China (grant No. 2012JQ1005), and Baoji University of Arts and Sciences Key Research Grant (grant Nos. ZK1032, ZK1033, ZK11060).

[1] A. Abdolvand, A. Podlipensky, S. Matthias, F. Syrowatka, U. Gösele, G. Seifert, and H. Graener, Adv. Mater. **17**, 2983 (2005).
[2] G. Maroulis, Chem. Phys. Lett. **444**, 44 (2007).
[3] A. Royon, K. Bourhis, M. Bellec, G. Papon, B. Bousquet, Y. Deshayes, T. Cardinal, and L. Canioni, Adv. Mat. **22**, 5282 (2010).
[4] S. Kumar, M. D. Bolan, and T. P. Bigioni, J. Am. Chem. Soc. **132**, 13141 (2010).
[5] L. Jensen, L. L. Zhao, and G. C. Schatz, J. Phys. Chem. C **111**, 4756 (2007).
[6] M. Pereiro, D. Baldomir, and J. E. Arias, Phys. Rev. A **75**, 63204 (2007).
[7] X. F. Tong, C. L. Yang, Y. P. An, M. S. Wang, X. G. Ma, and D. H Wang, J. Chem. Phys. **131**, 244304 (2009).
[8] J. S. Spendelow and A. Wieckowski, Phys. Chem. Chem. Phys. **9**, 2654 (2007).
[9] M. H. Rashid and T. K. Mandal, J. Phys. Chem. C **111**, 16750 (2007).
[10] G. M. Koretsky and M. B. Knickelbein, J. Chem. Phys. **107**, 10555 (1997).
[11] R. S. Eachus, A. P. Marchetti, and A. A. Muenter, Annu. Rev. Phys. Chem. **50**, 117 (1999).
[12] A. N. Lebedev and O. Stenzel, Eur. Phys. J. D **7**, 83 (1999).
[13] S.-H. Kim, G. Medeiros-Ribeiro, D. A. A. Ohlberg, R. S. Williams, and J. R. Heath, J. Phys. Chem. B **103**, 10341 (1999).
[14] X. Y. Gao, S. Y. Wang, J. Li, Y. X. Zheng, R. J. Zhang, P. Zhou, Y. M. Yang, and L. Y. Chen, Thin. Solid. Films. **455**, 438 (2004).
[15] V. Beutel, H. G. Krämer, G. L. Bhale, M. Kuhn, K. Weyers, and W. Demtröder, J. Chem. Phys. **98**, 2699 (1993).
[16] J. J. Scherer, J. B. Paul, C. P, Collier, and R. J. Saykally, J. Chem. Phys. **103**, 113 (1995).
[17] J. A. Howard, R. Sutcliffe, and B. Mile, J. Phys. Chem. **87**, 2268 (1983).

[18] M. Harb, F. Rabilloud, D. Simon, A. Rydlo, S. Lecoultre, F. Conus, V. Rodrigues, and C. Félix, J. Chem. Phys. **129**, 194108 (2008).
[19] V. Bonačić-Koutecký, L. Češpiva, P. Fantucci, and J. Koutecký, J. Chem. Phys. **98**, 7981 (1993).
[20] M. N. Huda and A. K. Ray, Phys. Rev. A **67**, 13201 (2003).
[21] V. E. Matulis, O. A. Ivashkevich, and V. S. Gurin, J. Mol. Struct. Theochem **664**, 291 (2010).
[22] R. Fournier, J. Chem. Phys. **115**, 2165 (2001).
[23] D. X. Tian, H. L. Zhang, and J. J. Zhao, Solid. State. Comm. **144**, 174 (2007).
[24] M. Pereiro, D. Baldomir, and J. E. Arias, Phys. Rev. A **75**, 63204 (2007).
[25] S. Lecoultre, A. Rydlo, J. Buttet, C. Félix, S. Gilb, and W. Harbich, J. Chem. Phys. **134**, 184504 (2011).
[26] M. Itoh, V. Kumar, T. Adschiri, and Y. Kawazoe, J. Chem. Phys. **131**, 174510 (2009).
[27] X. J. Hou, E. Janssens, P. Lievens, and M. T. Nguyen, Chem. Phys. **330**, 365 (2006).
[28] F. L. Liu and G. Jiang, J. Mol. Struct. Theochem **953**, 7 (2010).
[29] R. B. Dong, X. S. Chen, H. X. Zhao, X. F. Wang, H. B. Shu, Z. L. Ding, and L. Wei, J. Phys. B: At. Mol. Opt. Phys. **44**, 35102 (2011).
[30] M. Harb, F. Rabilloud, and D. Simon, J. Chem. Phys. **131**, 174302 (2009).
[31] G. F. Zhao and Z. Zeng, J. Chem. Phys. **125**, 14303 (2006).
[32] F. R. Negreiros, Z. Kuntová, G. Barcaro, G. Rossi, R. Ferrando, and A. Fortunelli, J. Chem. Phys. **132**, 234703 (2010).
[33] X. Y. Liu, Z. H. Zhu, and Y. Sheng, Chin. Phys. B **20**, 113101 (2011).
[34] M. J. Frisch, G. W. Trucks, H. B. Schlegel, G. E. Scuseria, M. A. Robb, J. R. Cheeseman, J. A. Montgomery, Jr., T. Vreven, K. N. Kudin, J. C. Burant, J. M. Millam, S. S. Iyengar, J. Tomasi, V. Barone, B. Mennucci, M. Cossi, G. Scalmani, N. Rega, G. A. Petersson, H. Nakatsuji, M. Hada, M. Ehara, K. Toyota, R. Fukuda, J. Hasegawa, M. Ishida, T. Nakajima, Y. Honda, O. Kitao, H. Nakai, M. Klene, X. Li, J. E. Knox, H. P. Hratchian, J. B. Cross, V. Bakken, C. Adamo, J. Jaramillo, R. Gomperts, R. E. Stratmann, O. Yazyev, A. J. Austin, R. Cammi, C. Pomelli, J. W. Ochterski, P. Y. Ayala, K. Morokuma, G. A. Voth, P. Salvador, J. J. Dannenberg, V. G. Zakrzewski, S. Dapprich, A. D. Daniels, M. C. Strain, O. Farkas, D. K. Malick, A. D. Rabuck, K. Raghavachari, J. B. Foresman, J. V. Ortiz, Q. Cui, A. G. Baboul, S. Clifford, J. Cioslowski, B. B. Stefanov, G. Liu, A. Liashenko, P. Piskorz, I. Komaromi, R. L. Martin, D. J. Fox, T. Keith, M. A. Al-Laham, C. Y. Peng, A. Nanayakkara, M. Challacombe, P. M. W. Gill, B. Johnson, W. Chen, M. W. Wong, C. Gonzalez, and J. A. Pople, Gaussian 03, Revision E.01; Gaussian, Inc., Wallingford CT 2004.
[35] J. Tao, J. P. Perdew, V. N. Staroverov, and G. E. Scueria, Phys. Rev. Lett. **91**, 146401 (2003).
[36] G. Maroulis, P. Karamanis, and C. Pouchan, J. Chem. Phys. **126**, 154316 (2007).
[37] P. Karamanis, C. Pouchan, and G. Maroulis, Phys. Rev. A **77**, 13201 (2008).
[38] G. Maroulis, J. Chem. Phys. **129**, 44314 (2008).
[39] P. J. Hay and W. R. Wadt, J. Chem. Phys. **82**, 299 (1985).
[40] R. Krishnan, J. S. Binkley, R. Seeger, and J. A. Pople, J. Chem. Phys. **72**, 650 (1980).
[41] K. P. Huber and G. Herzberg, Constants of Diatomic Molecules, Van Nostrand Reinhold, New York 1979.
[42] X Li, B. Kiran, and L. S. Wang, J. Phys. Chem. A **109**, 4366 (2005).
[43] J. Zhao, Y. Luo, and G. Wang, Eur. Phys. J. D **14**, 309 (2001).
[44] B. Kiran, X. Li, H. J. Zhai, L. F. Cui, and L. S. Wang, Angew. Chem. Int. Ed. **43**, 2125 (2004).
[45] Y. L. Cao, C. v. d. Linde, R. F. Höckendorf, and M. K. Beyer, J. Chem. Phys. **132**, 224307 (2010).
[46] G. Alameddin, J. Hunter, D. Cameron, and M. M. Kappes, Chem. Phys. Lett. **192**, 122 (1992).
[47] C. Jackschath, I. Rabin, and W. Schulz, Z. Phys. D **22**, 517 (1992).